Spectral line shape of nonresonant four-wave mixing in Markovian stochastic fields

R. Bratfalean and P. Ewart

Clarendon Laboratory, University of Oxford, Parks Road, Oxford OX1 3PU, United Kingdom

The spectral line shape of the four-wave mixing (FWM) signal, induced by broad bandwidth laser fields, is derived in the case of a nonresonant interaction. The laser fields are assumed to have a Lorentzian spectrum arising from Markovian stochastic fluctuations described by the phase-diffusion, chaotic field, and Gaussian-amplitude models. The usual ''phase conjugating'' geometry for FWM is considered where the nonresonant interaction is determined only by the statistics of, and the correlations between, the pump and probe fields. For each one of the four possible correlation states between the three input fields and for each of the three fluctuating field models, the line shape of the FWM signal is calculated and shown to be particularly sensitive to the field statistics. [S1050-2947(97)02709-1]

PACS number(s): 42.65.−k, 42.50.−p

I. INTRODUCTION

The electromagnetic waves emitted by lasers are subject to fluctuations of amplitude and phase that broaden the spectral bandwidth of the optical field. The spectral line shape of a light field is thus intimately related to its temporal coherence properties, which are in turn often determined by physical processes occurring in the source. Measurements of the intensity spectrum or line shape of the light are not usually sensitive to the field statistics since the phase information is lost in any measurement of intensity and the same spectral line shape may be presented by light fields having quite different statistics. On the other hand, measurements of the spectrum of light generated by a phase-sensitive process can distinguish between different types of statistical fluctuations in the field. The statistical properties of the light field are of particular importance for nonlinear optical processes since these are often sensitive to higher-order correlations in the fields [1]. The effects of such fluctuations have been studied in several nonlinear optical processes including resonance fluorescence [2], multiphoton absorption [3], multiphoton ionization [4], and stimulated Raman scattering [5]. Studies of two-photon absorption line shapes have allowed the dynamics of fluctuations in a phase-diffusing field to be distinguished [6].

Four-wave mixing (FWM) is a fruitful area for the study of field fluctuation effects where two pump fields and one probe field interact via the third-order susceptibility $\chi^{(3)}$ to generate the signal field. The signal intensity arising from the interaction of chaotic pump fields and a monochromatic probe has been calculated in the case where the pump bandwidth b was smaller than the atomic linewidth Γ of the medium [7]. The limit of very broad bandwidth lasers, where b exceeds Γ and all other relaxation rates in the problem, has been explored theoretically [8] and experimentally [9] to determine the signal dependence on the input laser intensity. This work was extended to calculate and to measure experimentally the temporal evolution of resonant degenerate four-wave mixing (DFWM) induced by pulsed, broad bandwidth fields [10]. These studies used the decorrelation approximation appropriate for very broad band fields and were not sensitive to the precise form of the statistics or to correlations in

the fields. Correlated fields in FWM have been considered in a number of other resonant situations such as weak fields [11] and time-delayed pulses [12,13]. Solutions have been found using decorrelation approximations or Monte Carlo methods [12,14].

The role of field fluctuations in FWM has been shown to be similar to that of dephasing collisions in that the destruction of interferences between coherent pathways by the collisions or fluctuations leads to extra resonances [15]. Such extra resonances are characterized by their appearance when none of the input frequencies (or combinations of them) is resonant with any transition from the initial atomic or molecular state [16]. The additional effect of correlations between the fluctuating fields also has been shown to lead to extra resonances [17,18] and is considered in a general treatment by Kofman, Levine, and Prior [19]. In this work the spectrum of a FWM signal is calculated when one or more of the input fields is broad and characterized by either Markovian or non-Markovian fluctuations. Although nonresonant, the input field frequencies lie close to the material resonances in the sense that the third-order susceptibility is frequency dependent in their spectral range [Eq. (3.1) of Ref. [19]]. The appearance of extra resonances, induced either by collisions or field fluctuations, arises from this frequency dependence of the third-order susceptibility. The destructive interference of coherent pathways is itself determined by the detuning of the input field frequencies from these material resonances. In the present work we consider a totally nonresonant situation and the medium response contains no resonant features. The effects on the observed spectrum then can depend only on the characteristics of the laser fields, and their correlations, if any.

The sensitivity of an atomic response to field statistics has been demonstrated so that an observable dependent on a resonant response can be used to distinguish between two statistically different field models [20]. A comparative study of resonant DFWM with chaotic and phase-diffusing fields has been presented in which the dependence of the signal intensity on the input intensity was calculated for each field model [21]. An alternative probe of the statistics is to measure the frequency spectrum of the signal generated in a nonlinear process. The measurement of the spectral line shape of a two-photon interaction to distinguish between different

characteristic time regimes of phase diffusion has been noted already [6]. The spectrum of broad bandwidth, resonant DFWM also has been studied theoretically for phase-diffusing fields using the decorrelation approximation [22,23] and validated by experimental measurement [23].

In this paper we describe the effects of different statistical models on the spectral line shape of the signal generated by *nonresonant* four-wave mixing. In previous work the spectral line shape of the signal wave was considered only in the case of resonant interaction between the light and the medium, i.e., the bandwidth of the driving fields encompassed a strong resonant transition frequency [21,22]. In this case the bandwidth of the generated FWM signal is strongly affected by the resonant enhancement of the medium's susceptibility. We present here a simple treatment of FWM line shapes generated by a nonresonant light-matter interaction, which indicates that measurement of such a spectrum is a potentially powerful technique for distinguishing between various types of field statistics.

By a nonresonant light-matter interaction we assume that the center laser frequency lies in a spectral region where the third-order susceptibility of the medium $\chi^{(3)}$ exhibits no selectivity. In the absence of medium resonances within the spectral bandwidth of the input light, a perturbation method may be used, provided also that we restrict the laser intensities to nonsaturating levels. The perturbation approach allows an expansion of the polarization in powers of the electric field, which is usually assumed to be *monochromatic*. However, in the case of a nonresonant interaction, *finite bandwidth* light fields may also be treated by this method. This approach is valid provided the optical coherence decay rate is fast, a condition that may be satisfied if either or both of two conditions are satisfied, viz., the transverse relaxation rate T_2 is short and/or the detuning from resonance is very large.

Such conditions are met, for example, where the nonresonant interaction takes place in the far wing of an atomic transition in the gas phase. In this case the detunings Δ_j ($j = 1,2,3$) of the three incident laser fields from the center line of the atomic transition must be much larger than the homogeneous width Γ if a flat medium response is to be experienced in the region of the laser frequency. Also the bandwidths b_j (full width at half maximum) and the Doppler width Δ_D should be much less than Δ_j.

In Sec. II of this paper a more detailed justification of the use of perturbation theory is given and the three statistical field models to be considered are outlined, viz., the phase-diffusion model (PDM), the chaotic field model (CFM), and the Gaussian-amplitude model (GAM) [24]. All three models provide a Lorentzian line shape and the finite bandwidth of the laser light is considered to arise from Markovian fluctuations of the complex amplitude of the field. In Sec. III we present the theoretical approach to be followed in deriving the frequency spectrum of the FWM signal in the particular case where all three input fields are *uncorrelated*. The effects on the signal line shape of correlations between the input fields are considered in Sec. IV for each of the three field models. Section V is devoted to conclusions.

II. PERTURBATION THEORY AND FIELD STATISTICS

We consider the case where the detunings of the incident fields Δ_j are much larger than Γ, b_j, and Δ_D and the differ-

ences between the detunings of the three input laser line centers are also much less than each Δ_j, so that the spectral response of the medium within the whole spectral range of the laser fields will be essentially flat. Thus every frequency within the spectral range of laser fields experiences the same third-order nonlinear susceptibility $\chi^{(3)}$. This condition is necessary to allow us to expand the polarization in powers of the electric field when the polarization is induced by an electric field of finite bandwidth. A further condition for the validity of the polarization expansion is that the incident fields are restricted to low intensities. We note that for larger Δ_j the upper limit of the allowed range of laser intensities is increased [25]. More details on the validity of this expansion of the polarization can be found in Ref. [25], p. 191, and [26], pp. 11–16.

We now describe the statistics of the input fluctuating fields, which are assumed to be governed by a Gaussian, stationary Markovian stochastic process [24]. We treat the fields classically and write them as

$$\mathbf{E}(x,t) = \underline{E}(x,t) + \text{c.c.} = E(x,t)\exp(-i\omega t + ikx) + \text{c.c.}$$
$$= \text{E}(t-x/c)\exp\{-i[\omega t + \phi(t-x/c) - kx]\} + \text{c.c.},$$
$$(1)$$

where

$$E(x,t) = E(t-x/c) = \text{E}(t-x/c)\exp[-i\phi(t-x/c)] \quad (2)$$

is the fluctuating complex amplitude of the field. $\text{E}(t-x/c)$ is its fluctuating modulus and $\phi(t-x/c)$ is its fluctuating phase. c is the speed of light in the medium for the angular frequency ω and wave vector k. The retardation effects in both the modulus and phase of the field complex amplitude are accounted for by the term x/c. We note that in relation (1) we have used the bold, the underlined, and the italic character in order to distinguish between the real electric field, the complex electric field, and the complex amplitude of the complex electric field, respectively. The normal character was used in Eqs. (1) and (2) to denote the modulus of the complex amplitude, which consequently is equal to half of the amplitude of the real field.

The mean value of $E(x,t)$ is assumed to be zero, $\langle E(x,t)\rangle = 0$, and its first-order correlation is exponential [24]:

$$\langle E(x_1,t_1)E^*(x_2,t_2)\rangle = \text{E}_0^2\exp\left[-\frac{b}{2}\left|(t_1-x_1/c)\right.\right.$$
$$\left.\left. -(t_2-x_2/c)\right|\right]. \quad (3)$$

b is the full width at half maximum of the Lorentzian spectrum. We can see by inspection that $\text{E}_0^2 = \langle \text{E}^2(t-x/c)\rangle$.

The form of the first-order correlation function, as expressed in Eq. (3), is a general feature of the three different stochastic models. As we shall see, this correlation function is sufficient for obtaining the signal line shape when the input laser fields are uncorrelated. Thus, in this uncorrelated case, the signal line shape will be the same for all three stochastic models. However, when dealing with correlated input laser fields the statistical features that characterize each

stochastic field must be considered. The individuality of each stochastic model resides in the marginal probability density and conditional probability density functions [24]. By use of these probability density functions we can calculate the correlation function of the fields in any order. In the four possible cases of correlated input fields we shall need to consider higher-order correlation functions in the derivation of the signal line shape. Specifically, in dealing with the case of all three fields being correlated we shall need to consider correlation functions up to third order. In contrast to the first-order correlation function, the higher-order correlation functions will be different for the three stochastic models. Therefore, for correlated input fields we shall have a different signal line shape for each stochastic model.

So we need to know the probability density functions and how they may be used to calculate higher-order correlation functions of the fields, $\langle E^N(x,t_1)E^{*N}(x,t_2)\rangle$. The line shape will be derived for all four possible cases of correlated input fields, but a detailed description of the mathematical calculations will be presented in only one of the four cases. We shall choose the case of correlated inputs fields that are uncorrelated with the probe field. In this case the required correlation functions may be reduced to products of first- and second-order correlation functions. Therefore, we shall be interested in the correlation functions for $N=1$ and 2. We first introduce the specific forms of the probability density functions for each field model and show how they may be used to derive the required higher-order correlation functions. In particular we shall calculate explicitly the second-order correlation function $\langle E^2(x,t_1)E^{*2}(x,t_2)\rangle$. A detailed description of the stochastic fields is given by Georges [24]. In what follows we shall recall only the salient features necessary for obtaining $\langle E^2(x,t_1)E^{*2}(x,t_2)\rangle$.

A. Phase-diffusion model

In the PDM we have a constant modulus of the complex amplitude, but the phase of the complex amplitude undergoes a continuous random walk [27–29]. For this stochastic model the average $\langle E^N(x_1,t_1)E^{*N}(x_2,t_2)\rangle$ can be written as (see details in Appendix A)

$$\langle E^N(x_1,t_1)E^{*N}(x_2,t_2)\rangle = E_0^{2N}\exp\left[-N^2\frac{b}{2}|(t_1-x_1/c)\right.$$
$$\left.-(t_2-x_2/c)|\right]. \quad (4)$$

B. Chaotic field model

In the CFM the complex amplitude of the field $E(x,t)$ can be written as the sum of two independent Gaussian stochastic real amplitudes that are 90° out of phase. So $E(x,t) = E_a(x,t) + iE_b(x,t)$, where $E_a(x,t)$ and $E_b(x,t)$ are independent Gaussian stochastic processes with zero mean and equal variance. For this stochastic model the average $\langle E^N(x_1,t_1)E^{*N}(x_2,t_2)\rangle$ can be written as (see details in Appendix B)

$$\langle E^N(x_1,t_1)E^{*N}(x_2,t_2)\rangle = N!E_0^{2N}\exp\{-Nb[(t_1-x_1/c)$$
$$-(t_2-x_2/c)]/2\}. \quad (5)$$

C. Gaussian-amplitude model

The Gaussian-amplitude field has a complex amplitude that has no imaginary part, so it is modeled by a real Gaussian stochastic amplitude with zero mean. Thus we may note that $E(x,t) = E(t-x/c)$, where in this case $E(t-x/c)$ is no longer a modulus but a real quantity allowed to fluctuate in both positive and negative regions. For this stochastic model the average $\langle E^2(x_1,t_1)E^{*2}(x_2,t_2)\rangle$ can be written as (see details in Appendix C)

$$\langle E^2(x_1,t_1)E^{*2}(x_2,t_2)\rangle = E_0^2(1+2\exp\{-b[(t_1-x_1/c)$$
$$-(t_2-x_2/c)]\}). \quad (6)$$

The general expression of $\langle E^N(x_1,t_1)E^{*N}(x_2,t_2)\rangle$ can be calculated following the iterative method of complete mathematical induction. However, we shall stop here because, as we previously mentioned, we are interested in $\langle E^N(x_1,t_1)E^{*N}(x_2,t_2)\rangle$ only for $N=1$ and 2.

III. THEORY OF BROAD BANDWIDTH, NONRESONANT, FWM LINE SHAPE

We consider the standard ''phase conjugating'' arrangement for FWM consisting of counterpropagating pump fields interacting with a probe field crossing at a small angle. The input fields will be described by the statistical models outlined above, which have a Lorentzian line shape. Then, for the particular case when the probed medium is a gas, we shall take into account the atomic motion by considering one well-defined velocity class of atoms. We shall find the expressions of the light fields in the rest frame of these atoms, use these expressions to derive the induced polarization of the medium, and then translate this polarization back to the laboratory frame. We shall show that the polarization, and hence the signal line shape, will not be influenced by atomic motion in this nonresonant interaction. The strength of the signal field is then calculated by integration of the polarization along the interaction length L. We then calculate the field autocorrelation function, which, by use of the Wiener-Khintchine theorem, will provide the frequency spectrum of the signal wave. The line shape of the FWM signal will be calculated first for the case of *uncorrelated* input fields. The result for *correlated* input fields will be calculated in detail only for the case of correlated pump fields. The results for other combinations of correlations between pump and probe fields will be presented without showing the details of the calculations.

A. Atomic motion

We take the incident laser beams to propagate along the x axis and the electric fields to be linearly polarized, parallel to the y axis. We further assume that they are not depleted on propagating through the interaction region. The fields will be expressed in the most general form of relation (1); $\mathbf{E}_1(x,t)$ and $\mathbf{E}_2(x,t)$ are the pump fields and $\mathbf{E}_3(x,t)$ is the probe field:

$$\mathbf{E}_1(x,t) = \underline{E}_1(x,t) + \text{c.c.} = E_1(t - x/c_1)$$
$$\times \exp\{-i[\omega_1 t + \phi_1(t - x/c_1) - k_1 x]\} + \text{c.c.,} \tag{7}$$

$$\mathbf{E}_2(x,t) = \underline{E}_2(x,t) + \text{c.c.} = E_2(t - x/c_2)$$
$$\times \exp\{-i[\omega_2 t + \phi_2(t - x/c_2) - k_2 x]\} + \text{c.c.,} \tag{8}$$

$$\mathbf{E}_3(x,t) = \underline{E}_3(x,t) + \text{c.c.} = E_3(t - x/c_3)$$
$$\times \exp\{-i[\omega_3 t + \phi_3(t - x/c_3) - k_3 x]\} + \text{c.c.} \tag{9}$$

All quantities in Eqs. (7)–(9) are defined in the laboratory frame. So x is the coordinate along the interaction region defined in the laboratory frame.

Now we shall include the effects of atomic motion for the particular case of a gaseous medium. We consider first only one class of atoms having a well-defined velocity v and the electric fields in the rest frame of these moving atoms. If we denote by x' the coordinate along the interaction region in the frame of the moving atom then the transformation relation between x and x' will be

$$x = x' + v \cdot t, \tag{10}$$

where v is the velocity of the molecule, which is assumed not to be relativistic. Substituting Eq. (10) into Eqs. (7)–(9), we find the electric fields in the frame of the moving atoms:

$$\mathbf{E}_1'(x',t) = \underline{E}_1'(x',t) + \text{c.c.} = E_1[t(1 - v/c_1) - x'/c_1]$$
$$\times \exp(-i\{(\omega_1 - k_1 v)t + \phi_1[t(1 - v/c_1)$$
$$- x'/c_1] - k_1 x'\}) + \text{c.c.,} \tag{11}$$

$$\mathbf{E}_2'(x',t) = \underline{E}_2'(x',t) + \text{c.c.} = E_2[t(1 - v/c_2) - x'/c_2]$$
$$\times \exp(-i\{(\omega_2 - k_2 v)t + \phi_2[t(1 - v/c_2)$$
$$- x'/c_2] - k_2 x'\}) + \text{c.c.,} \tag{12}$$

$$\mathbf{E}_3'(x',t) = \underline{E}_3'(x',t) + \text{c.c.} = E_3[t(1 - v/c_3) - x'/c_3]$$
$$\times \exp(-i\{(\omega_3 - k_3 v)t + \phi_3[t(1 - v/c_3)$$
$$- x'/c_3] - k_3 x^r\}) + \text{c.c.} \tag{13}$$

As we have noted previously, the polarization of the medium can be expanded in a power series of the total electric-field strength. Therefore, in the rest frame of the moving atoms, the polarization of the medium will be

$$\mathbf{P}'(x',t) = \chi^{(1)}\mathbf{E}'(x',t) + \chi^{(2)}\mathbf{E}'^2(x',t) + \chi^{(3)}\mathbf{E}'^3(x',t)$$
$$+ \cdots, \tag{14}$$

where

$$\mathbf{E}'(x,t) = \mathbf{E}_1'(x',t) + \mathbf{E}_2'(x',t) + \mathbf{E}_3'(x',t). \tag{15}$$

In Eq. (15) we have not included the signal beam as it is assumed to be weak relative to the input fields. This is par-

ticularly true in dilute media, where the absorption of the input beams is also negligible. Then the polarization term, responsible for the FWM signal generation, will be given by

$$\mathbf{P}_4'(x',t) = \underline{P}_4'(x',t) + \text{c.c.} = \chi^{(3)}\underline{E}_1'(x',t)\underline{E}_2'(x',t)[\underline{E}_3'(x',t)]^*$$
$$+ \text{c.c.} \tag{16}$$

The electric-field strength in the laboratory frame is derived from the third-order nonlinear polarization, in the same (laboratory) frame, by substituting x' into Eq. (16) by $x - vt$ according to Eq. (10). This gives

$$\mathbf{P}_4(x,t) = \underline{P}_4(x,t) + \text{c.c.} = \chi^{(3)}\underline{E}_1(x,t)\underline{E}_2(x,t)[\underline{E}_3(x,t)]^*$$
$$+ \text{c.c.,} \tag{17}$$

a result that is independent of the atomic velocity.

The conclusion is that there is no distinction between the induced polarization of two classes of atoms of different velocities in the laboratory frame. The physical argument supporting this conclusion is based on our assumption that the medium response is the same whether or not the frequency domain of the input lasers is shifted within a Doppler width. The mathematical translation of the above statement consists in putting the same third-order susceptibility in both relations (16) and (17), which refer to the moving molecular frame and laboratory frame, respectively. Therefore, within the validity of perturbation theory, in the case of our nonresonant light-medium interaction, the signal frequency spectrum will not be affected by atomic motion or the associated Doppler broadening. This result distinguishes the nonresonant case from the resonant interaction where the line shape of broad bandwidth FWM was found to involve the convolution of a homogeneous line shape with the square of the Doppler-broadened line profile [23].

B. FWM line shape for uncorrelated fields

The polarization $\underline{P}_4(x,t)$ acts as a source term in the nonlinear wave equation leading to a signal field strength

$$\underline{E}_4(x,t) = E_4(x,t)\exp\{-i[\omega_4 t - k_4 x]\}, \tag{18}$$

where the angular frequency of the signal wave is

$$\omega_4 = \omega_1 + \omega_2 - \omega_3 \tag{19}$$

and the signal wave vector is

$$k_4 = (\omega_1 + \omega_2 - \omega_3)/c_4 = \omega_4/c_4. \tag{20}$$

We denote by c_j the velocity in the medium of the input pump, $j = 1, 2$; probe, $j = 3$; and signal, $j = 4$. Using the slowly varying envelope approximation integration of the space derivative of $E_4(x,t)$ along the interaction length yields the generated signal field strength $E_4(L,t)$ (details are given in Appendix D),

$$E_4(L,t) = C \int_0^L E_1(t - x/c_1) E_2(t - x/c_2)$$
$$\times E_3^*(t - x/c_3)\exp(i\Delta k x)dx, \tag{21}$$

where C is a complex constant and Δk is the wave-vector mismatch, both of which are defined in Appendix D.

In order to derive the frequency spectrum of the signal wave we need first to form its autocorrelation $\Gamma(L,\tau)$, where L indicates that we are interested in the signal emerging from the end of the interaction region. This autocorrelation will be defined as [30]

$$\Gamma(L,\tau)=\lim_{T\to\infty}\frac{1}{2T}\int_{-T}^{T}\underline{E}_4(L,t+\tau)[\underline{E}_4(L,t)]^*dt \quad (22)$$

or

$$\Gamma(L,\tau)=\langle\underline{E}_4(L,t+\tau)[\underline{E}_4(L,t)]^*\rangle, \quad (23)$$

where the angular brackets in relation (23) indicate that an average must be performed over the fluctuations of the fields.

Using Eqs. (18) and (21), relation (23) can be written again as

$$\Gamma(L,\tau)=(CC^*)\exp(-i\omega_4\tau)\int_0^L\int_0^L\{dx\,dx'\langle E_1(t+\tau$$
$$-x/c_1)E_2(t+\tau-x/c_2)E_3^*(t+\tau-x/c_3)$$
$$\times E_1^*(t-x'/c_1)E_2^*(t-x'/c_2)E_3(t-x'/c_3)\rangle$$
$$\times\exp[i\Delta k(x-x')]\}. \quad (24)$$

In the case where the three input beams are uncorrelated the average in the integrand in Eq. (24) can be written as a product of three averages, leading to the result

$$\langle E_1(t+\tau-x/c_1)E_2(t+\tau-x/c_2)E_3^*(t+\tau-x/c_3)E_1^*(t-x'/c_1)E_2^*(t-x'/c_2)E_3(t-x'/c_3)\rangle$$

$$=\langle E_1(t+\tau-x/c_1)E_1^*(t-x'/c_1)\rangle\langle E_2(t+\tau-x/c_2)E_2^*(t-x'/c_2)\rangle\langle E_3^*(t+\tau-x/c_3)E_3(t-x'/c_3)\rangle$$

$$=E_{01}^2E_{02}^2E_{03}^2\exp\left[-\frac{\left(b_1\left|\tau-\dfrac{x-x'}{c_1}\right|+b_2\left|\tau-\dfrac{x-x'}{c_2}\right|+b_3\left|\tau-\dfrac{x-x'}{c_3}\right|\right)}{2}\right], \quad (25)$$

where b_j, $j=1,2,3$, indicates the bandwidths of each individual field. The last equality in Eq. (25) is based on relation (3). Substituting Eq. (25) into Eq. (24), we get the expression for the autocorrelation

$$\Gamma(L,\tau)=E_{01}^2E_{02}^2E_{03}^2(CC^*)\exp(-i\omega_4\tau)$$

$$\times\int_0^L\int_0^L\left\{dxdx'\,\exp\left[-\frac{\left(b_1\left|\tau-\dfrac{x-x'}{c_1}\right|+b_2\left|\tau-\dfrac{x-x'}{c_2}\right|+b_3\left|\tau-\dfrac{x-x'}{c_3}\right|\right)}{2}+i\Delta k(x-x')\right]\right\}. \quad (26)$$

In what follows we consider the coherence length of the laser L_c to be much longer than the interaction length L. This is the case for most FWM experiments with the exception of those multiplexing techniques using very broad bandwidth lasers [31]. So, since $L_c\gg L$, we can neglect the retardation effects along the interaction length. This basically means that $1\gg b_i(x-x')/c_i$ for every x and x' in the interaction region. Therefore, the final frequency spectrum will not be significantly altered if we set $(x-x')/c_i$ equal to zero in every modulus in Eq. (26). So Eq. (26) may be written as

$$\Gamma(L,\tau)=D\,\exp(-i\omega_4\tau)\exp\{-[(b_1+b_2+b_3)|\tau|/2]\}, \quad (27)$$

where

$$D=E_{01}^2E_{02}^2E_{03}^2(CC^*)\int_0^L\int_0^L\{dx\,dx'\exp[-i\Delta k(x-x')]\}. \quad (28)$$

Conversely, when $L_c\ll L$, retardation effects along the interaction length can no longer be neglected. Besides altering the FWM signal dependence on L [32] it is likely also that the

frequency spectrum will be altered. So, in what follows we consider only the case $L_c\gg L$.

Now that we have the autocorrelation of the signal wave, given in Eq. (27), we may calculate its power spectral density by use of the Wiener-Khintchine theorem as

$$P(\omega)=\int_{-\infty}^{\infty}\Gamma(L,\tau)\exp(i\omega\tau)d\tau. \quad (29)$$

Substituting Eq. (27) into Eq. (29) we obtain

$$P(\omega)=D\int_{-\infty}^{\infty}\exp[i(\omega-\omega_4)\tau]\exp$$

$$\times[-(b_1+b_2+b_3)|\tau|/2]d\tau. \quad (30)$$

The integrand in the above integral will have an odd imaginary part so the spectral power density will yield a real quantity and relation (30) may be written

$$P(\omega) = D \int_{-\infty}^{\infty} \cos[(\omega - \omega_4)\tau]$$
$$\times \exp[-(b_1 + b_2 + b_3)|\tau|/2]d\tau. \quad (31)$$

This integral may be evaluated [33] to yield the spectral power density of the signal wave

$$P(\omega) = 2D \frac{b/2}{(b/2)^2 + (\omega - \omega_4)^2}, \quad (32)$$

where

$$b = b_1 + b_2 + b_3. \quad (33)$$

So, according to Eq. (31), in the uncorrelated case the line shape of the signal wave is a Lorentzian centered on $\omega_4 = \omega_1 + \omega_2 - \omega_3$ and of bandwidth equal to the sum of the bandwidths of the input fields. This result is valid whichever stochastic model is used to describe the statistics of the fields since, in relation (25), we used only the first-order correlation function, which is the same for all three stochastic models.

C. FWM line shape for correlated fields

The three input waves in a FWM process may be correlated in one of four possible ways: one case when all the fields are correlated and three when only two of the fields are correlated. We present a complete calculation of the signal wave line shape for all three models of stochastic field in only one of these four correlation cases, viz., where the forward and backward pump fields are fully correlated (no delay) and both are uncorrelated with the probe. Thus $\omega_1 = \omega_2$ and $b_1 = b_2$. For the other three correlated cases we shall present only the results as the mathematical procedure is the same. We maintain the assumption made when dealing with the uncorrelated fields, i.e., $L \ll L_c$. Therefore, we shall ignore all retardation terms in the complex amplitudes.

1. Correlated pump fields uncorrelated with the probe field

(a) Phase-diffusion model. For this case relation (25) takes the form

$$\langle E_1(t+\tau)E_2(t+\tau)E_3^*(t+\tau)E_1^*(t)E_2^*(t)E_3(t)\rangle$$
$$= E_{02}^2/E_{01}^2 \langle E_1^2(t+\tau)E_1^{*2}(t)\rangle \langle E_3^*(t+\tau)E_3(t)\rangle$$
$$= E_{01}^2 E_{02}^2 E_{03}^2 \exp\{-[(4b_1+b_3)|\tau|/2]\}, \quad (34)$$

where in the last equality of relation (34) we have used relation (4). Now we just have to follow the standard calculation procedure described by relations (25)–(32) in order to see that the line shape of the signal wave will be given by the relation

$$P_{\text{PDM}(1,2)}(\omega) = 2D \frac{(4b_1+b_3)/2}{[(4b_1+b_3)/2]^2 + (\omega - \omega_4)^2}. \quad (35)$$

So the line shape is a Lorentzian with a bandwidth equal to $(b_1 + b_2 + b_3) + 2b_1$, which is larger than that of the uncorrelated case by the addition of $2b_1$.

(b) Chaotic field model. In this case relation (25) becomes

$$\langle E_1(t+\tau)E_2(t+\tau)E_3^*(t+\tau)E_1^*(t)E_2^*(t)E_3(t)\rangle$$
$$= E_{02}^2/E_{01}^2 \langle E_1^2(t+\tau)E_1^{*2(t)}\rangle \langle E_3^*(t+\tau)E_3(t)\rangle$$
$$= 2E_{01}^2 E_{02}^2 E_{03}^2 \exp\{-[(2b_1+b_3)|\tau|/2]\}, \quad (36)$$

where in the second equality of Eq. (36) we have used relation (5). Now we simply follow the same calculation procedure described by relations (25)–(32) and arrive at the relation

$$P_{\text{CFM}(1,2)}(\omega) = 4D \frac{(2b_1+b_3)/2}{[(2b_1+b_3)/2]^2 + (\omega - \omega_4)^2}. \quad (37)$$

So the line shape is a Lorentzian with a bandwidth equal to $2b_1 + b_3 = (b_1 + b_2 + b_3)$, which is the same result as in the case of the uncorrelated fields.

(c) Gaussian-amplitude model. For the GAM, relation (25), in this case of correlated fields, becomes

$$\langle E_1(t+\tau)E_2(t+\tau)E_3^*(t+\tau)E_1^*(t)E_2^*(t)E_3(t)\rangle$$
$$= E_{02}^2/E_{01}^2 \langle E_1^2(t+\tau)E_1^{*2}(t)\rangle \langle E_3^*(t+\tau)E_3(t)\rangle$$
$$= E_{01}^2 E_{02}^2 E_{03}^2 [1 + 2\exp(-b_1|\tau|)][\exp(-b_3|\tau|/2)]$$
$$= E_{01}^2 E_{02}^2 E_{03}^2 \{\exp(-b_3|\tau|/2)$$
$$+ 2\exp[-(2b_1+b_3)|\tau|/2]\}, \quad (38)$$

where in the second equality of Eq. (38) we have used relation (6). Again following the standard calculation procedure described by relations (25)–(31), we find that the line shape of the signal wave will be given by the relation

$$P_{\text{GAM}(1,2)}(\omega) = 4D \frac{(2b_1+b_3)/2}{[(2b_1+b_3)/2]^2 + (\omega - \omega_4)^2}$$
$$+ 2D \frac{b_3/2}{(b_3/2)^2 + (\omega - \omega_4)^2}. \quad (39)$$

So the line shape is the sum of two Lorentzians of different bandwidths and different magnitudes.

The normalized line shapes of nonresonant broadband FWM calculated for each stochastic field model are shown in Fig. 1 for the case of correlated pump fields. The result in the case of all fields being uncorrelated is also shown for comparison. We see that the line shape for the CFM is identical in both the correlated and uncorrelated cases. However, the result for the PDM shows a larger bandwidth in the correlated case, whereas the GAM yields a narrower line in the correlated case relative to the uncorrelated case. The differences are even more dramatic when the bandwidth of the probe is narrower than that of the pumps. This situation is illustrated in Fig. 2 for the case of correlated pumps that are uncorrelated with a probe that has a linewidth 10 times narrower than the pumps.

Using the above procedure, we can calculate the signal line shape for the other cases of correlated input laser fields. We quote the results below and, for the sake of an overall picture, we present again the case we have just detailed.
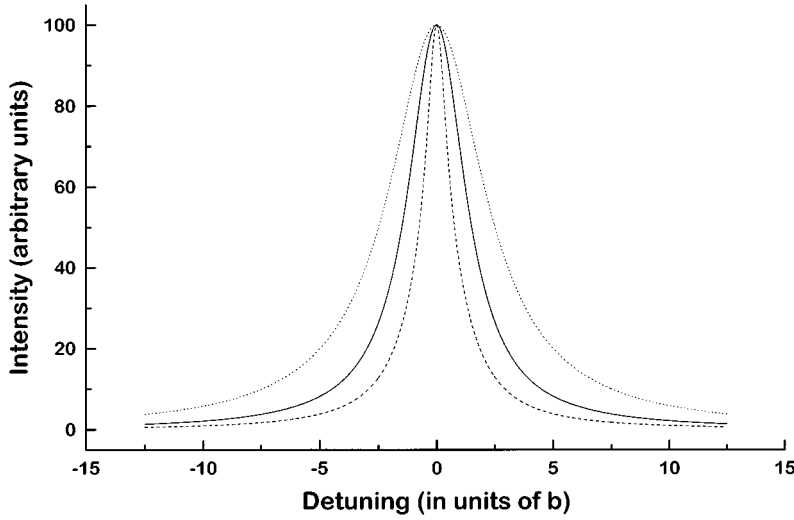
FIG. 1. Normalized FWM signal line shapes in the case of correlated pump fields, uncorrelated with the probe for each stochastic model: PDM, dotted line; CFM, dot-dashed line; GAM, dashed line, when all the input laser fields have equal bandwidths $b_1 = b_2 = b_3 = b$. The line shape for uncorrelated input laser fields (solid line) is displayed for reference and overlies the CFM curve.

2. Correlated pump fields uncorrelated with the probe field

This implies $\omega_1 = \omega_2$ and $b_1 = b_2$:

$$P_{\mathrm{PDM}(1,2)}(\omega) = 2D\,\frac{(4b_1 + b_3)/2}{[(4b_1 + b_3)/2]^2 + (\omega - \omega_4)^2}, \quad (40)$$

$$P_{\mathrm{CFM}(1,2)}(\omega) = 4D\,\frac{(2b_1 + b_3)/2}{[(2b_1 + b_3)/2]^2 + (\omega - \omega_4)^2}, \quad (41)$$

$$P_{\mathrm{GAM}(1,2)}(\omega) = 4D\,\frac{(2b_1 + b_3)/2}{[(2b_1 + b_3)/2]^2 + (\omega - \omega_4)^2}$$
$$+ 2D\,\frac{b_3/2}{(b_3/2)^2 + (\omega - \omega_4)^2}. \quad (42)$$

The normalized line shapes of Eqs. (40)–(42) are shown graphically in Fig. 1 for the case where $b_1 = b_2 = b_3 = b$ and in Fig. 2 for the case where $b_1 = b_2 = 10b$ and $b_3 = b$.

3. Forward pump and probe fields correlated and uncorrelated with the backward pump field

This implies $\omega_1 = \omega_3$ and $b_1 = b_3$:

$$P_{\mathrm{PDM}(1,3)}(\omega) = 2D\,\frac{b_2/2}{(b_2/2)^2 + (\omega - \omega_4)^2}, \quad (43)$$

$$P_{\mathrm{CFM}(1,3)}(\omega) = 2D\,\frac{(2b_1 + b_2)/2}{[(2b_1 + b_2)/2]^2 + (\omega - \omega_4)^2}$$
$$+ 2D\,\frac{b_2/2}{(b_2/2)^2 + (\omega - \omega_4)^2}, \quad (44)$$

$$P_{\mathrm{GAM}(1,3)}(\omega) = 4D\,\frac{(2b_1 + b_2)/2}{[(2b_1 + b_2)/2]^2 + (\omega - \omega_4)^2}$$
$$+ 2D\,\frac{b_2/2}{(b_2/2)^2 + (\omega - \omega_4)^2}. \quad (45)$$

The normalized line shapes of Eqs. (43)–(45) are shown graphically in Fig. 3 for the case where $b_1 = b_2 = b_3 = b$.
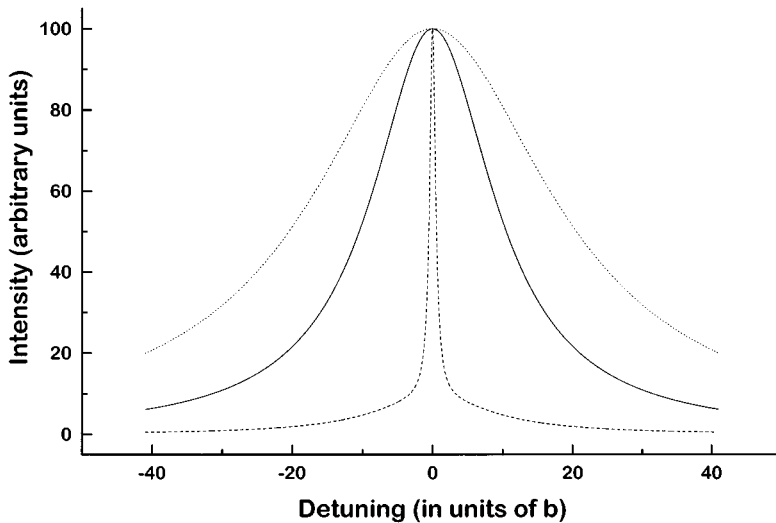

FIG. 2. Normalized FWM signal line shapes in the case of correlated pump fields, uncorrelated with the probe for each stochastic model: PDM, dotted line; CFM, dot-dashed line; GAM, dashed line, when the pump bandwidth is 10 times the probe bandwidth $b_1 = b_2 = 10b$ and $b_3 = b$. The line shape for uncorrelated input laser fields (solid line) is displayed for reference and overlies the CFM curve.
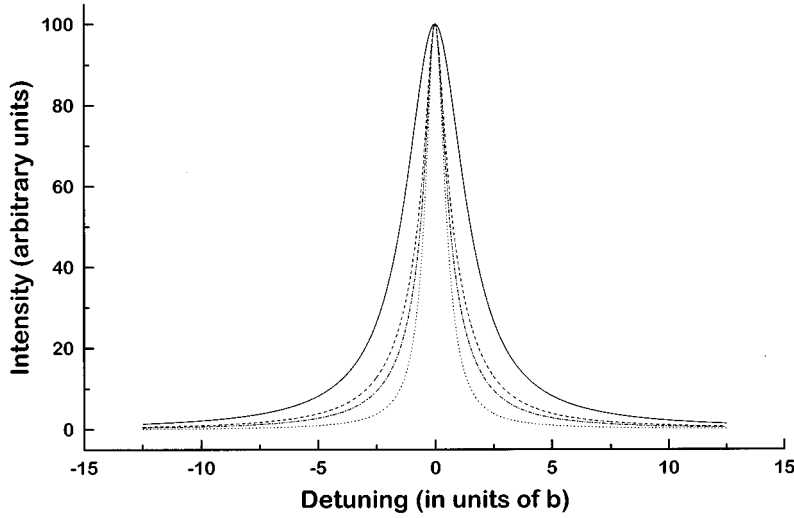
FIG. 3. Normalized FWM signal line shapes in the case of the forward (backward) pump correlated with the probe and uncorrelated with the backward (forward) field for each stochastic model: PDM, dotted line; CFM, dot-dashed line; GAM, dashed line, when all the input laser fields have equal bandwidths $b_1=b_2=b_3=b$. The line shape for uncorrelated input laser fields (solid line) is displayed for reference.

4. Backward pump and probe fields correlated and uncorrelated with the forward pump field

This implies $\omega_2=\omega_3$ and $b_2=b_3$:

$$P_{\text{PDM(2,3)}}(\omega)=2D\,\frac{b_1/2}{(b_1/2)^2+(\omega-\omega_4)^2},\qquad(46)$$

$$P_{\text{CFM(2,3)}}(\omega)=2D\,\frac{(2b_2+b_1/2)}{[(2b_2+b_1)/2]^2+(\omega-\omega_4)^2}$$
$$+2D\,\frac{b_1/2}{(b_1/2)^2+(\omega-\omega_4)^2},\qquad(47)$$

$$P_{\text{GAM(2,3)}}(\omega)=4D\,\frac{(2b_2+b_1)/2}{[(2b_2+b_1)/2]^2+(\omega-\omega_4)^2}$$
$$+2D\,\frac{b_1/2}{(b_1/2)^2+(\omega-\omega_4)^2}.\qquad(48)$$

The normalized line shapes of Eqs. (46)–(48) are also shown graphically in Fig. 3 for the case where $b_1=b_2=b_3=b$. We note that the results are the same when either one of the pump fields, forward or backward, is correlated with the probe and uncorrelated with the other pump.

5. All three fields are correlated

This implies $\omega_1=\omega_2=\omega_3$ and $b_1=b_2=b_3$:

$$P_{\text{PDM(1,2,3)}}(\omega)=2D\,\frac{b_2/2}{(b_2/2)^2+(\omega-\omega_4)^2},\qquad(49)$$

$$P_{\text{CFM(1,2,3)}}(\omega)=4D\,\frac{3b_1/2}{(3b_1/2)^2+(\omega-\omega_4)^2}$$
$$+8D\,\frac{b_1/2}{(b_1/2)^2+(\omega-\omega_4)^2},\qquad(50)$$

$$P_{\text{GAM(1,2,3)}}(\omega)=12D\,\frac{3b_1/2}{(3b_1/2)^2+(\omega-\omega_4)^2}$$
$$+18D\,\frac{b_1/2}{(b_1/2)^2+(\omega-\omega_4)^2}.\qquad(51)$$

The normalized line shapes of Eqs. (49)–(51) are shown graphically in Fig. 4 for the case where $b_1=b_2=b_3=b$.
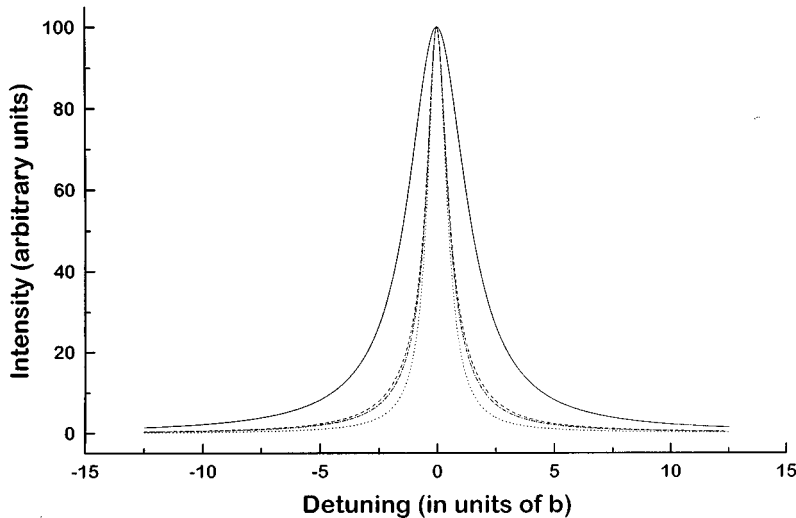

FIG. 4. Normalized signal line shapes in the case of all three input fields correlated for each stochastic model: PDM, dotted line; CFM, dot-dashed line; GAM, dashed line, when all the input laser fields have equal bandwidths $b_1=b_2=b_3=b$. The line shape for uncorrelated input laser fields (solid line) is displayed for reference.

D. Integrated signal magnitude

The integrated signal magnitude is obtained by integrating the spectral power density along the frequency axis from $-\infty$ to $+\infty$. We denote by I_0 the integrated signal magnitude in the case of uncorrelated input fields. We find that in any case where only two of the three input laser fields are correlated, the integrated signal magnitude is equal to I_0 for the PDM, $2I_0$ for the CFM, and $3I_0$ for the GAM. In the case where all the three input laser fields are correlated, the integrated signal magnitude is equal to I_0 for the PDM, $6I_0$ for the CFM, and $15I_0$ for the GAM. It is easy to verify that the value of the integrated signal magnitude, in terms of I_0, is equal to half the sum of the coefficients of D in the expression of the signal line shape as given by relations (40)–(51).

IV. DISCUSSION

The results of the calculations presented here show clearly the influence of the field statistics on the line shape of nonresonant four-wave mixing. It is more difficult to get a clear picture of the physical origins of the effects in each case of correlated fields and each type of fluctuating field. However, some insight may be gained by considering the case of the phase-diffusion model. The electric field in the PDM may be considered to be a single frequency with an instantaneous value $\omega(t)$ that varies in time around an average value $\langle \omega(t) \rangle$. Now let us consider for simplicity a FWM process where the input waves have the same average frequency $\langle \omega_i(t) \rangle = \langle \omega_j(t) \rangle$, $i,j=1,2,3$. However, the instantaneous frequencies $\omega_i(t)$ and $\omega_j(t)$ are equal only when the i,j fields are correlated. The instantaneous signal frequency is

$$\omega_4(t) = \omega_1(t) + \omega_2(t) - \omega_3(t). \tag{52}$$

When the three input fields are *uncorrelated* it is easy to show that the signal bandwidth $b_4 = b_1 + b_2 + b_3$ since any frequency within the band of one field can couple equally with all frequencies in another band. When one of the fields is correlated with either or both of the other input fields then the range of possible signal frequencies is constrained. Consider the case of the probe correlated with the forward pump, i.e., $\omega_1(t) = \omega_3(t)$. Then clearly $\omega_2(t) = \omega_4(t)$ and the range of the values of the signal is the same as that of the backward pump, i.e., b_2. This is the result given in Eq. (43).

Similarly, when the backward pump and probe are correlated $\omega_2(t) = \omega_3(t)$ and $\omega_1(t) = \omega_4(t)$ and we obtain the result given in Eq. (46). When all input fields are correlated $\omega_1(t) = \omega_2(t) = \omega_3(t)$ and so $\omega_4(t) = \omega_2(t)$ and again the signal bandwidth $b_4 = b_2$, which is the result in Eq. (49).

The case of correlated pumps and an uncorrelated probe requires careful consideration. For uncorrelated pumps and an uncorelated probe (i.e., all fields uncorrelated) the result may be written as

$$b_4 = 2b_1 + b_3. \tag{53}$$

The signal bandwidth is the result of adding the probe bandwidth b_3 to the sum frequency bandwidth $2b_1$. In the correlated pumps case the result is

$$b_4 = 4b_1 + b_3, \tag{54}$$

i.e., the sum frequency bandwidth $(\omega_1 + \omega_2)$ is twice the result for the uncorrelated pumps. In the uncorrelated pump case we consider a given instantaneous frequency in one pump beam to be $\langle \omega \rangle + \Delta \omega$, where $\Delta \omega$ is some random detuning within the bandwidth b_1. This frequency may couple with any frequency within the bandwidth of the second pump. However, the most probable value of this second pump frequency is $\langle \omega \rangle$ giving a signal frequency

$$\omega_S = 2 \langle \omega \rangle + \Delta \omega. \tag{55}$$

In the correlated pump case the second pump frequency is constrained to be the same as the first and must therefore be detuned also by $\Delta \omega$. Thus

$$\omega_S = 2 \langle \omega \rangle + 2 \Delta \omega. \tag{56}$$

The frequency excursions of the sum frequency in the correlated case are thus twice that in the uncorrelated case. Hence the bandwidth of the sum frequency of correlated pumps is twice that of uncorrelated pumps, i.e., $4b_1$ rather than $2b_1$, and we obtain the result of Eq. (54), which validates Eq. (40).

V. CONCLUSION

We have considered the effect of field statistics on the spectral line shape of nonresonant FWM induced by broad bandwidth lasers that have a Lorentzian spectrum. Using a perturbation approach, the line shape has been calculated for fields whose statistics belong to one of the three Markovian stochastic models considered: the phase-diffusion model, the chaotic field model, and the Gaussian-amplitude model. Provided that the nonresonant condition is satisfied for all frequencies within the input laser bandwidth, the signal is found to be unaffected by atomic motion and hence by Doppler broadening. This contrasts with the result for resonant degenerate FWM where the line shape involves a convolution with the square of the Doppler profile [23].

The spectral line shapes of the FWM signal were calculated in the limit where the laser coherence length L_c exceeds the interaction length L. For uncorrelated input fields the line shape of the signal wave is found to be independent of the precise form of the statistics. In this case the result is simply a Lorentzian centered on the signal frequency $\omega_4 = \omega_1 + \omega_2 - \omega_3$, with a bandwidth equal to the sum of the bandwidths of the input fields. However, for correlated input fields the signal line shape is found to depend on the statistics and to be sensitive to the type of correlations between the input laser fields.

The rather trivial result obtained in the case of uncorrelated laser fields is maintained only in the CFM and only in the case of correlated pump beams that are uncorrelated with the probe beam. In this specific correlation case the signal wave bandwidth is larger in the PDM and in the GAM the line shape is no longer a Lorentzian but the sum of two Lorentzians of different bandwidths and magnitudes. Results for the other possible correlations between the pump and probe fields have been derived.

The most important conclusion of this paper, expressed by the results in relations (40)–(51), is that nonresonant four-wave mixing allows distinctions to be made between differ-

ent kinds of fluctuation statistics in the light field if correlated input fields are used. In practice it should be possible to detect these effects by measuring the signal line shape and controlling the degree of correlation between pump and probe fields by time delays or polarization state. Methods to distinguish between different field statistics have been proposed that mostly use resonant single-photon or multiphoton interactions [19,20]. We note that the method proposed here involves a fully nonresonant interaction and so the results are potentially less complicated by the dynamics of stationary atomic or molecular states. It is also worth pointing out that, in principle, the statistics of a pulsed laser field could be determined by measurements on a single laser pulse. The experimental requirement would be that the spectrum of the FWM signal be resolved on a given pulse and this could be achieved, for example, by use of a charge coupled device camera to record an interferogram produced by a high-resolution Fabry-Pérot interferometer. Experiments to demonstrate this possibility are currently planned in our laboratory.

It has been proposed recently that correlations between longitudinal modes of laser fields may be probed by time-delayed FWM experiments that measure the pulse autocorrelation function [34]. Finally, we note that the mathematical procedure we have used in this paper could be used to derive the signal line shapes of other nonresonant, nonlinear optical processes.

APPENDIX A

Considering relation (2), the complex amplitude of the field in the PDM can be written as

$$E(x,t) = E_0 \exp[-i\phi(t-x/c)], \tag{A1}$$

where E_0 is a positive real quantity that can easily be identified with E_0 from relation (3). The marginal probability density is given by

$$f(\phi,t) = e^{-\phi^2/2bt}/\sqrt{2\pi bt} \tag{A2}$$

and the conditional probability density is given by

$$f(\phi_1,t_1|\phi_2,t_2)$$
$$= \exp\left[-\frac{(\phi_1-\phi_2)^2}{2b(t_1-t_2)}\right] / \sqrt{2\pi b(t_1-t_2)},$$
$$t_1 > t_2. \tag{A3}$$

The average $\langle E^N(x,t_1)E^{*N}(x,t_2)\rangle$, where N is a natural number, can be calculated using the marginal probability density and the conditional probability density as [24]

$$\langle E^N(x,t_1)E^{*N}(x,t_2)\rangle = \int_{-\infty}^{\infty} d\phi_2 f(\phi_2,t_2) \int_{-\infty}^{\infty} d\phi_1 f(\phi_1,t_1|\phi_2,t_2)E^N(x,t_1)E^{*N}(x,t_2) = E_0^{2N}\exp\left[-N^2\frac{b}{2}|(t_1-t_2)|\right]. \tag{A4}$$

In relation (A4) we have assumed that the average is calculated at $x=x_1=x_2$. If x_1 and x_2 are different then formally we have to replace, in relation (A4), t_1 by t_1-x_1/c and t_2 by t_2-x_2/c. Then relation (A4) will become

$$\langle E^N(x_1,t_1)E^{*N}(x_2,t_2)\rangle = E_0^{2N}\exp\left[-N^2\frac{b}{2}|(t_1-x_1/c)-(t_2-x_2/c)|\right]. \tag{A5}$$

APPENDIX B

The marginal probability density and the conditional probability density can be expressed in terms of the fluctuating modulus of the complex amplitude and fluctuating field phase as defined by relation (2). The marginal probability density is given by

$$f(E,\phi) = E e^{-E^2/E_0^2}/(\pi E_0^2) \tag{B1}$$

and the conditional probability density is given by

$$f(E_1,\phi_1,t_1|E_2,\phi_2,t_2) = \left[E_1\exp\left(-\frac{E_1^2+r^2E_2^2-2rE_1E_2\cos(\phi_1-\phi_2)}{E_0^2(1-r^2)}\right)\right] / [\pi E_0^2(1-r^2)], \tag{B2}$$

where $r=\exp[-b/2(t_1-t_2)]$ is the correlation coefficient, E_1 is the modulus of the complex amplitude at time t_1, and E_2 is the modulus of the complex amplitude at time t_2. ϕ_1 and ϕ_2 are the instantaneous values of the fluctuating phase at times t_1 and t_2, respectively. In order to perform the average of the type $\langle E^N(x,t_1)E^{*N}(x,t_2)\rangle$, where N is a natural number, we note that the conditional probability density is related to the associated Laguerre polynomials as [24]

$$\int_0^{2\pi} d\phi_1 \int_0^\infty dE_1 \left[L_N^m\left(\frac{E_1^2}{E_0^2}\right)\right] E_1^m[\exp(-im\phi_1)]\, f(E_1,\phi_1,t_1|E_2,\phi_2,t_2) = \{\exp[-(2N+m)b(t_1-t_2)/2]\}\left[L_N^m\left(\frac{E_2^2}{E_0^2}\right)\right] E_2^m$$

$$\times \exp(-im\phi_2), \qquad (B3)$$

where $L_N^m(x)$ is the associated Laguerre polynomial. N and m are natural numbers. Considering the form of these polynomials [33,34] and setting $N=0$, Eq. (B3) becomes

$$\int_0^{2\pi} d\phi_1 \int_0^\infty dE_1 E_1^m[\exp(-im\phi_1)]\, f(E_1,\phi_1,t_1|E_2,\phi_2,t_2) = \{\exp[-mb(t_1-t_2)/2]\} E_2^m \exp(-im\phi_2). \qquad (B4)$$

The average $\langle E^N(x,t_1)E^{*N}(x,t_2)\rangle$ is performed in a similar manner to Eq. (A4) and taking into account Eq. (B4) we obtain

$$\langle E^N(x,t_1)E^{*N}(x,t_2)\rangle = \int_0^\infty dE_2 \int_0^{2\pi} d\phi_2 \cdot f(E_2,\phi_2) \int_0^\infty dE_1 \int_0^{2\pi} d\phi_1\, f(E_1,\phi_1,t_1|E_2,\phi_2,t_2) E^N(x,t_1)E^{*N}(x,t_2)$$

$$= \{\exp[-Nb(t_1-t_2)/2]\}\int_0^\infty dE_2 \int_0^{2\pi} d\phi_2\, f(E_2,\phi_2)E_2^{2N} = N! E_0^{2N}\{\exp[-Nb(t_1-t_2)/2]\}. \qquad (B5)$$

If $t_1=t_2$ we obtain a well-known relation for the CFM [24], which is

$$\langle E^N(x,t_1)E^{*N}(x,t_2)\rangle = N!\langle E(x,t)E^*(x,t)\rangle^N,$$

and so Eq. (B5) is verified.

In relation (B5) we have assumed that the average is calculated at $x=x_1=x_2$. If x_1 and x_2 are different then we have to replace, in relation (B5), t_1 by t_1-x_1/c and t_2 by t_2-x_2/c. Then relation (B5) will become

$$\langle E^N(x_1,t_1)E^{*N}(x_2,t_2)\rangle = N! E_0^{2N}\exp\{-Nb[(t_1-x_1/c)$$
$$-(t_2-x_2/c)]/2\}. \qquad (B6)$$

APPENDIX C

The marginal probability density is given by

$$f(E)=Ee^{-E^2/2E_0^2}/\sqrt{2\pi E_0^2} \qquad (C1)$$

and the conditional probability density is given by

$$f(E_1,t_1|E_2,t_2)=\left[\exp\left(-\frac{(E_1-rE_2)^2}{2E_0^2(1-r^2)}\right)\right] \Big/ \sqrt{2\pi E_0^2(1-r^2)}, \qquad (C2)$$

where E_1 is the real amplitude at time t_1 and E_2 the real amplitude at time t_2. In order to perform the average of the type $\langle E^N(x,t_1)E^{*N}(x,t_2)\rangle$, where N is a natural number, we use the fact that the conditional probability density is related to Hermite polynomials as [24]

$$\int_{-\infty}^\infty dE_1 \left[H_N\left(\frac{E_1}{\sqrt{2E_0^2}}\right)\right] f(E_1,t_1|E_2,t_2)$$

$$= \{\exp[-Nb(t_1-t_2)/2]\}\left[H_N\left(\frac{E_2}{\sqrt{2E_0^2}}\right)\right]. \qquad (C3)$$

Considering the form of Hermite polynomials [33,34] and setting $N=1$ in Eq. (C3), we obtain

$$\int_{-\infty}^\infty dE_1\, E_1\, f(E_1,t_1|E_2,t_2) = E_2\exp[-b(t_1-t_2)/2]. \qquad (C4)$$

So, as in the derivation of Eq. (A4), the correlation function $\langle E(x,t_1)E^*(x,t_2)\rangle$ will be given by

$$\langle E(x,t_1)E^*(x,t_2)\rangle$$

$$= \int_{-\infty}^\infty dE_2\, E_2\, f(E_2) \int_{-\infty}^\infty dE_1\, E_1\, f(E_1,t_1|E_2,t_2)$$

$$= \exp[-b(t_1-t_2)/2]\int_{-\infty}^\infty dE_2\, E_2^2\, f(E_2)$$

$$= E_0^2\exp[-b(t_1-t_2)/2], \qquad (C5)$$

where for the second equality in Eq. (C5) we have used Eq. (C4).

Now in evaluating the average $\langle E^2(x,t_1)E^{*2}(x,t_2)\rangle$ we shall start with relation (C3), where we shall consider $N=2$. Then we obtain

$$\int_{-\infty}^{\infty} d\mathrm{E}_1 \left[2\left(\frac{\mathrm{E}_1^2}{\mathrm{E}_0^2}\right) - 2 \right] f(\mathrm{E}_1,t_1|\mathrm{E}_2,t_2)$$

$$= \left[2\left(\frac{\mathrm{E}_2^2}{\mathrm{E}_0^2}\right) - 2 \right] \exp[-b(t_1-t_2)] \qquad (C6)$$

or

$$\int_{-\infty}^{\infty} d\mathrm{E}_1 \, \mathrm{E}_1^2 \, f(\mathrm{E}_1,t_1|\mathrm{E}_2,t_2) = \mathrm{E}_0^2 + (\mathrm{E}_2^2 - \mathrm{E}_0^2)\exp[-b(t_1-t_2)],$$
$$(C7)$$

where in deriving Eq. (C7) we have used the fact that

$$\int_{-\infty}^{\infty} d\mathrm{E}_1 \, f(\mathrm{E}_1,t_1|\mathrm{E}_2,t_2) = 1, \qquad (C8)$$

which can be obtained from Eq. (C3) by setting $N=0$.

Now, as before, we can calculate $\langle E^2(x,t_1)E^{*2}(x,t_2)\rangle$ in the same way as for relation (A4), obtaining

$$\langle E^2(x,t_1)E^{*2}(x,t_2)\rangle$$

$$= \int_{-\infty}^{\infty} d\mathrm{E}_2 \, f(\mathrm{E}_2) \int_{-\infty}^{\infty} d\mathrm{E}_1 \, (\mathrm{E}_1\mathrm{E}_2)^2 \, f(\mathrm{E}_1,t_1|\mathrm{E}_2,t_2)$$

$$= \int_{-\infty}^{\infty} d\mathrm{E}_2 \, f(\mathrm{E}_2) \, \mathrm{E}_2^2\{\mathrm{E}_0^2 + (\mathrm{E}_0^2 - \mathrm{E}_0^2)\exp[-b(t_1-t_2)]\}$$

$$= \mathrm{E}_0^2\{1 + 2\exp[-b(t_1-t_2)]\}, \qquad (C9)$$

where in deriving the second equality in Eq. (C9) we have used relation (C7). The result in Eq. (C9) can be verified by setting $t_1 = t_2$, which for $N=2$ yields the particular form of the usual relation for the GAM [24]:

$$\langle E^N(x,t_1)E^{*N}(x,t_2)\rangle = [1 \times 3 \times \cdots \times (2N-1)]$$
$$\times \langle E(x,t_1)E^*(x,t_2)\rangle^N.$$

In relation (C9) we have assumed that the average is calculated at $x=x_1=x_2$. If x_1 and x_2 are different then formally we have to replace, in relation (C9), t_1 by $t_1 - x_1/c$ and t_2 by $t_2 - x_2/c$. Then relation (C9) will become

$$= \langle E^2(x_1,t_1)E^{*2}(x_2,t_2)\rangle = \mathrm{E}_0^2(1 + 2\exp\{-b[(t_1-x_1/c)$$

$$- (t_2 - x_2/c)]\}). \qquad (C10)$$

APPENDIX D

We start with the nonlinear wave equation

$$\nabla^2 \mathbf{E}_4(x,t) - \frac{1}{c^2}\frac{\partial^2}{\partial t^2}\mathbf{E}_4(x,t) = \mu_0 \frac{\partial^2}{\partial t^2}\mathbf{P}_4(x,t), \quad (D1)$$

where the source polarization term $\mathbf{P}_4(x,t)$ arises from the third-order nonlinear response of the medium to the three input fields

$$\mathbf{P}_4(x,t) = \chi^{(3)}\mathrm{E}_1(t-x/c_1)\mathrm{E}_2(t-x/c_2)\mathrm{E}_3^*(t-x/c_3)$$

$$\times \exp\{-i[\omega_4 t - (k_1+k_2-k_3)x]\} + \mathrm{c.c.}$$
$$(D2)$$

and $\mathbf{E}_4(x,t)$ can be written, using the least restrictive form, as

$$\mathbf{E}_4(x,t) = \underline{E}_4(x,t) + \mathrm{c.c.} = E_4(x,t)\exp\{-i[\omega_4 t - k_4 x]\} + \mathrm{c.c.},$$
$$(D3)$$

where by $E_4(x,t)$ we denote the fluctuating complex amplitude of $\underline{E}_4(x,t)$. The optical angular frequency of the FWM signal is

$$\omega_4 = \omega_1 + \omega_2 - \omega_3. \qquad (D4)$$

We substitute Eqs. (D3) and (D2) into Eq. (D1) and perform the derivatives over space and time. On the right-hand side of Eq. (D1) we neglect the time derivatives arising from the product $\mathrm{E}_1(t-x/c_1)\mathrm{E}_2(t-x/c_2)\mathrm{E}_3^*(t-x/c_3)$ relative to that arising from the frequency term ($\omega_4 t$) since the rate of fluctuation-induced change in $\mathbf{P}_4(x,t)$ is much smaller than the optical frequency. For the same reason, on the left-hand side of Eq. (D1) we neglect time derivatives of $E_4(x,t)$ with respect to time derivatives of $\exp(-i\omega_4 t)$. After doing these calculations we multiply both sides of the resulting equation by $\exp(-i\omega_4 t)$. Then, using the slowly varying envelope approximation, we arrive at the final result

$$2ik_4 \left[\frac{\partial}{\partial x} E_4(x,t) \right] \exp(ik_4 x) + \mathrm{c.c.}$$

$$= -\mu_0 \omega_4^2 \chi(3)\mathrm{E}_1(t-x/c_1)\mathrm{E}_2(t-x/c_2)\mathrm{E}_3^*(t-x/c_3)$$

$$\times \exp[i(k_1+k_2-k_3)x] + \mathrm{c.c.} \qquad (D5)$$

Hence

$$\frac{\partial}{\partial x} E_4(x,t) = -\frac{\mu_0 \omega_4^2 \chi^{(3)}}{2ik_4}$$

$$\times \frac{\mathrm{E}_1(t-x/c_1)\mathrm{E}_2(t-x/c_2)\mathrm{E}_3^*(t-x/c_3)}{\exp[-i(k_1+k_2-k_3-k_4)x]}.$$
$$(D6)$$

We denote by C the constant

$$C \equiv -\frac{\mu_0 \omega_4^2 \chi^{(3)}}{2ik_4} \qquad (D7)$$

and the wave-vector mismatch

$$\Delta k \equiv k_1 + k_2 - k_3 - k_4. \qquad (D8)$$

Substituting Eqs. (D7) and (D8) into Eq. (D6) and integrating along the interaction region, assuming that $E_4(x,t)=0$ for $x=0$, we finally get the generated signal field in the form

$$E_4(L,t) = C \int_0^L dx \, \mathrm{E}_1(t-x/c_1)\mathrm{E}_2(t-x/c_2)\mathrm{E}_3^*(t-x/c_3)$$

$$\times \exp(i\Delta k x), \qquad (D9)$$

which is identical to relation (21).

[1] P. Lambropolous, Phys. Rev. **168**, 1418 (1968); B. R. Mollow, *ibid.* **175**, 1555 (1968).

[2] G. S. Agarwal, Phys. Rev. A **1**, 1445 (1970); P. Zoller and P. Lambropolous, J. Phys. B **13**, 69 (1980).

[3] N. C. Wong and J. H. Eberly, Opt. Lett. **1**, 211 (1977).

[4] J. L. F. de Mejiere and J. H. Eberly, Phys. Rev. A **17**, 1416 (1978).

[5] R. L. Carman, F. Shimuzu, C. S. Wang, and N. Bloembergen, Phys. Rev. A **2**, 60 (1970); A. Akhmanov, Yu. E. D'Yakav, and L. I. Pavlov, Zh. Eksp. Teor. Fiz. **66**, 520 (1974) [Sov. Phys. JETP **39**, 249 (1974)].

[6] D. S. Elliott, M. W. Hamilton, K. Arnett, and S. J. Smith, Phys. Rev. Lett. **53**, 439 (1984).

[7] R. Saxena and G. S. Agarwal, Opt. Lett. **8**, 566 (1983).

[8] G. Alber, J. Cooper, and P. Ewart, Phys. Rev. A **21**, 2344 (1985); J. Cooper, A. Charlton, D. R. Meacher, P. Ewart, and G. Alber, *ibid.* **40**, 5705 (1989).

[9] D. R. Meacher, A. Charlton, P. Ewart, J. Cooper, and G. Alber, Phys. Rev. A **42**, 3018 (1990).

[10] M. Kaczmarek, D. R. Meacher, and P. Ewart, J. Mod. Opt. **37**, 1561 (1990).

[11] G. S. Agarwal, Phys. Rev. A **37**, 4741 (1988).

[12] P. Tchenio, A. Debarrer, J.-C. Keller, and J.-L. Le Gouet, Phys. Rev. A **39**, 1970 (1989); Phys. Rev. Lett. **62**, 415 (1989).

[13] V. Finkelstein and P. R. Berman, Phys. Rev. A **42**, 3145 (1990).

[14] G. Vemuri, G. S. Agarwal, R. Roy, M. H. Anderson, J. Cooper, and S. J. Smith, Phys. Rev. A **44**, 6009 (1991).

[15] G. S. Agarwal and C. V. Kunasz, Phys. Rev. A **27**, 996 (1983).

[16] Y. Prior, A. Bogdan, M. Dagenais, and N. Bloembergen, Phys. Rev. Lett. **46**, 111 (1981).

[17] Y. Prior, I. Schek, and J. Jortner, Phys. Rev. A **31**, 3775 (1985).

[18] G. S. Agarwal, C. V. Kunasz, and J. Cooper, Phys. Rev. A **36**, 143 (1987).

[19] A. G. Kofman, A. M. Levine, and Y. Prior, Phys. Rev. A **37**, 1248 (1988).

[20] Th. Haslwanter, H. Ritsch, J. Cooper, and P. Zoller, Phys. Rev. A **38**, 5652 (1988); H. Ritsch, P. Zoller, and J. Cooper, Phys. Rev. A **41**, 2653 (1990).

[21] G. S. Agarwal, G. Vemuri, C. V. Kunasz, and J. Cooper, Phys. Rev. A **46**, 5879 (1992).

[22] D. R. Meacher, P. G. R. Smith, and P. Ewart, Phys. Rev. A **46**, 2718 (1992).

[23] P. G. R. Smith and P. Ewart, Phys. Rev. A **54**, 2347 (1996).

[24] A. T. Georges, Phys. Rev. A **21**, 6 (1980).

[25] R. W. Boyd, *Nonlinear Optics* (Academic, San Diego, 1992).

[26] *Optical Phase Conjugation*, edited by Robert A. Fisher (Academic, San Diego, 1983).

[27] Athanasios Papoulis, *Probability, Random Variables and Stochastic Processes*, 3rd ed. (McGraw-Hill, New York, 1991).

[28] Mary L. Boas, *Mathematical Methods in the Physical Sciences*, 2nd ed. (Wiley, New York, 1983).

[29] *Handbook of Mathematical Functions*, Natl. Bur. Stand. Appl. Math. Ser. No. 55, edited by M. Abramowitz and I. A. Stegun (U.S. GPO, Washington, DC, 1964).

[30] Max Born and Emil Wolf, *Principles of Optics*, 6th ed. (Pergamon, Oxford, 1980).

[31] P. Ewart and P. Snowdon, Opt. Lett. **15**, 1403 (1990).

[32] R. Bratfalean and P. Ewart, J. Mod. Opt. **43**, 2523 (1996).

[33] I. S. Gradsteyn and I. M. Ryzhik, *Table of Integrals, Series and Products*, edited by A. Jeffrey (Academic, New York, 1965).

[34] M. Belsley, M. Kaczmarek, and P. Ewart (unpublished).